Potassium currents in adult rat intracardiac neurones

Sylvia X. Xi-Moy and N. J. Dun*

Department of Anatomy and Neurobiology, Medical College of Ohio, 3000 Arlington Avenue, Toledo, OH 43614, USA

1. Properties of K^+ currents were studied in isolated adult rat parasympathetic intracardiac neurones with the use of single-electrode voltage-clamp techniques.

2. A hyperpolarization-activated inward rectifier current was revealed when the membrane was clamped close to the resting level (−60 mV). The slowly developing inward relaxation had a mean amplitude of 450 pA at −150 mV, an activation threshold of −60 to −70 mV and a relaxation time constant of 41 ms at −120 mV. The current was reversibly blocked by Cs^+ (1 mM) and became smaller with reduced $[K^+]_o$ and $[Na^+]_o$, indicating that this inward rectifier current probably is a time- and voltage-dependent Na^+–K^+ current.

3. Step depolarizations from the holding potential of −80 mV evoked a transient (< 100 ms at −40 mV) outward K^+ current (I_A) which was blocked by 4-aminopyridine (4-AP, 1 mM). The time constants for I_A inactivation were 20 ms at −50 mV and 16 ms at −20 mV. The steady-state activation and (removal of) inactivation curve showed a small overlap between −70 and −40 mV; the reversal potential of I_A was close to E_K.

4. Step hyperpolarizations from the depolarized potentials, i.e. −30 mV, revealed a slow inward relaxation associated with the deactivation of a time- and voltage-dependent current. The inward relaxation became faster at more hyperpolarized potentials and reversed at −85 and −53 mV in 4·7 and 15 mM $[K^+]_o$. This current was blocked by muscarine (20 μM) and Ba^{2+} (1 mM) but not affected by Cs^+ (1 mM); this current may correspond to the M-current (I_M).

5. Depolarization-activated outward K^+ currents were evoked by holding the membrane close to the resting potential in the presence of tetrodotoxin (TTX, 3 μM), 4-AP (1 mM) and Ba^{2+} (1 mM). The amplitude of the outward relaxation and the tail current became smaller as the $[K^+]_o$ was elevated. The outward tail current was reduced in a Ca^{2+}-free solution and the residual current was eliminated by the addition of tetraethylammonium (TEA, 10 mM); the reversal potential was shifted in a direction predicted by the Nernst equation. These findings suggest the presence of delayed rectifier K^+ current and Ca^{2+}-activated K^+ current.

6. Superfusion of TEA, Ba^{2+} and 4-AP, but not Cs^+, induced rhythmic discharges in some of the otherwise quiescent intracardiac neurones.

7. It is concluded that several K^+ conductances are present in adult rat intracardiac neurones and these currents working in concert endow the neurones with a multitude of mechanisms to ensure proper membrane excitability and firing pattern.

Vagal regulation of cardiac functions, e.g. automaticity, conductivity and contractility, has long been recognized and extensively studied (Randall, 1984). Parasympathetic intracardiac ganglia are the essential pathway through which vagal cardiac efferents modulate the activity of cardiac tissues. Anatomical studies of the mammalian heart have revealed plexuses of parasympathetic ganglia and interganglionic nerves located mainly in atrial subepicardium; some are also located in the interatrial septum (Malor, Taylor, Chesher & Griffin, 1974; Randall, 1984; Burkholder, Chambers, Hotmire, Wurster, Moody & Randall, 1992). The location and topography of these ganglia, which innervate specific targets, e.g. sino-atrial node or atrio-ventricular node, remain fairly constant among different animals (Randall, 1984; Moravec & Moravec, 1984; Burkholder *et al.* 1992).

* To whom correspondence should be addressed.

Each mammalian intracardiac ganglion consists of tens to hundreds of cells which receive synaptic inputs from the vagus nerve and, in turn, project their axons to different cardiac tissues (Randall, 1984). Several types of neurones can be distinguished within the intracardiac ganglia on the basis of their morphology, electrical activity and transmitter phenotype (Xi, Randall & Wurster, 1991*a*, *b*; Selyanko, 1992). These include cholinergic principal neurones; interneurones; adrenergic, small, intensely fluorescent (SIF) cells; and various peptidergic neurones reported from different species (Malor *et al.* 1974; Weihe, Reinecke & Forssmann, 1984; Hassall & Burnstock, 1986; Xi *et al.* 1991*a*).

To date, there have been relatively few voltage-clamp studies of the ionic conductances underlying the neuronal excitability of mammalian intracardiac neurones. A recent patch-clamp study explored the ionic basis of the resting membrane potential and voltage-sensitive K^+ currents in cultured intracardiac neurones derived from neonatal rats (Xu & Adams, 1992). The present study was undertaken to explore the characteristics of K^+ currents and their possible physiological activities in adult, mammalian intracardiac neurones.

Some of the work has been published in an abstract (Xi-Moy & Dun, 1992).

METHODS

Experiments were performed on intracardiac ganglia isolated from 4- to 5-week-old Sprague–Dawley rats of either sex.

Dissection and localization of ganglia

Animals were anaesthetized with ketamine-HCl (80 mg kg^{-1}, I.P.). The hearts, with attached great vessel roots, were rapidly removed and rinsed with Krebs solution at 4 °C. Hearts were mounted in a Sylgard-lined culture dish and examined epicardially under a dissecting microscope (× 40) using direct fibre-optic illumination.

Ganglia with surrounding adipose tissues and underlying subepicardial myocardium were carefully dissected from the heart. The preparation was then pinned to the tissue bath with the outer side of the fat pad facing up and superfused with Krebs solution maintained at 34 °C. The size of the preparations was approximately 1·0 mm in length and 0·2 mm in depth. For exposing the embedded ganglia, connective tissues were carefully removed from the surface with fine scissors. To preserve the synaptic inputs to ganglionic neurones, the attached interganglionic nerves were left undisturbed.

A dorsal view of the rat heart is shown in Fig. 1. Four fat pads, containing several ganglia interconnected by fine vagal branches, can be easily identified. Because of their relatively large size and fixed location, two of the ganglia (marked by stars) were most frequently selected for the present study: the one in the junction of right precava, right atrium and right pulmonary vein and the other in the junction between left pulmonary vein and left atrium close to the superior and dorsal portion of the interatrial septum.

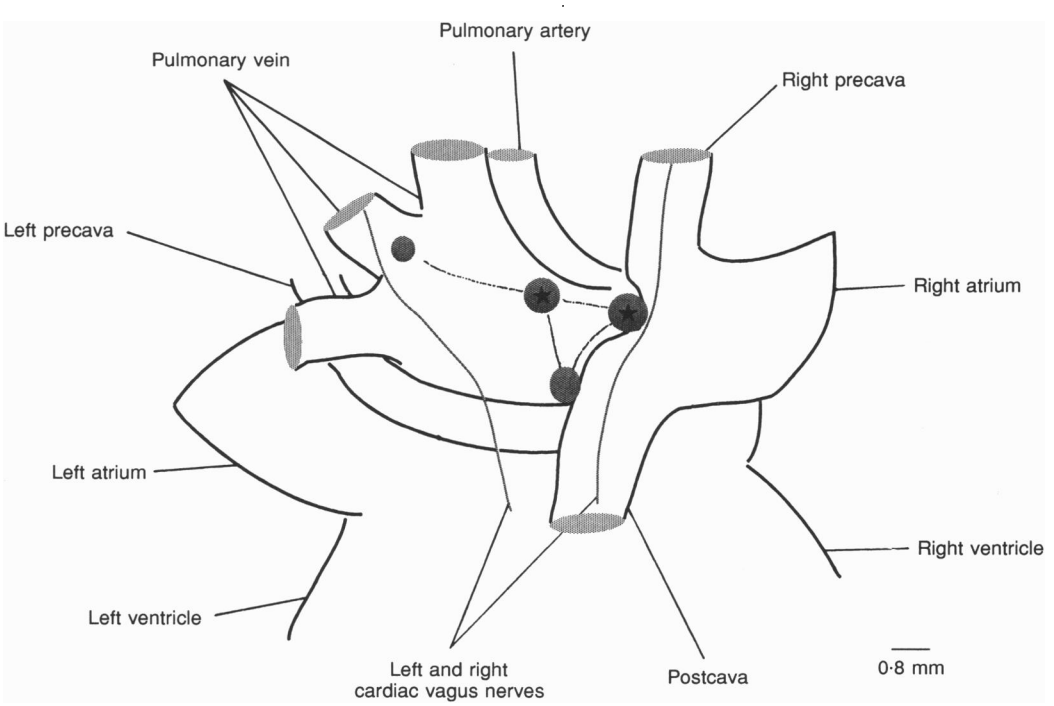

Figure 1. Schematic diagram of epicardial distribution of intracardiac ganglia on the dorsal view of adult rat atria

Round, shaded areas represent the ganglia with their surrounding adipose tissues. Two of them (marked with stars) were most frequently selected for the present study. Interganglionic nerves were seen running between areas containing the ganglia.

Electrophysiological recording and data analysis

Intracardiac neurones were current or voltage clamped using the single-electrode current- and voltage-clamp techniques. Fibre-filled borosilicate glass electrodes (1·2 mm o.d., 0·6 mm i.d.; Sutter Instrument Co.) were pulled on a Narishige horizontal pipette puller. Electrodes were filled with 3 M KCl (DC resistance, 30–40 MΩ) and mounted on a micromanipulator. Superfused ganglia were visualized using a dissecting microscope (×40) and direct fibre-optic illumination. Impalement was achieved by manually advancing the electrode and transiently oscillating the capacity neutralization. The electrode was connected to the headstage of a sample-and-hold voltage-clamp preamplifier (Axoclamp-2A). The switching frequency was between 3 and 5 kHz and the duty cycle was 30%. The clamp gain was between 2 and 4 nA mV^{-1} and the filtering frequency was 3 kHz. The headstage output was continuously monitored with a separate oscilloscope. Before voltage-clamp study, the optimal capacitance neutralization was carefully achieved by advancing the capacitance neutralization control until the monitored waveform decayed most rapidly to a horizontal baseline without any overshoot. The cell membrane potential was held at its resting level and the gain was increased as far as possible without causing instability in the response to a −10 mV step command. The clamp settling time to step changes of membrane potential was within 5 ms. The capacity transients were minimized by reducing the level of superfusing solution to less than 0·3 mm above the tissue. Voltage-clamp protocols were generated by two synchronized pulse generators (Grass S88) connected to the preamplifier. Two separate rectangular pulses could be summed as desired from the holding potential. Protocols for each series of experiments will be described in the text. Voltage and current responses were monitored on a digital oscilloscope (Nicolet 310) and saved to disk and a chart recorder (Gould RS 3200) for later analysis. A digital plotter (HP 7475A) was used for off-line data display.

When estimating membrane conductance, the amplitude of membrane currents evoked by step commands of 500 ms duration was plotted as a function of command potentials. The steady-state currents were measured at the off-set of the 500 ms voltage command. Due to the presence of transient currents at the beginning of the voltage command, the instantaneous currents, estimated by extrapolating the currents measured after achieving voltage control (about 5 ms), had decayed back to the level at time zero (Allen & Burnstock, 1990*b*).

Solutions and drugs

All solutions were made using double distilled water from Milli-Q Water System (Millipore) and analytical grade chemicals. The Krebs solution used had the following composition (mM): NaCl, 117; KCl, 4·7; $MgCl_2$, 1·2; $NaHCO_3$, 25; NaH_2PO_4, 1·2; $CaCl_2$, 2·5; and glucose, 11; gassed with 95%O_2–5%CO_2 (pH 7·4). In preparing low-$[Ca^{2+}]_o$ Krebs solution, Ca^{2+} was replaced isosmotically by $MgCl_2$. Increases in $[K^+]_o$ were made by isosmotic replacement of NaCl with KCl. In preparing Na^+-free solution, NaCl, $NaHCO_3$ and NaH_2PO_4 were isosmotically replaced by Tris base (titrated with HCl, pH 7·4).

Unless otherwise mentioned, drugs and chemicals were from Sigma Chemical Co. The drugs used were tetrodotoxin (TTX), 4-aminopyridine (4-AP), $BaCl_2$ (J. T. Baker Chemical Co., Phillipsburg, NJ, USA), CsCl, $CdCl_2$, hexamethonium bromide, (±)-muscarine chloride, and tetraethylammonium chloride (TEA). All drugs in known concentrations were applied by superfusion.

Data are expressed as means ± S.E.M. for n cells tested.

RESULTS

Results described below were obtained from more than 150 parasympathetic intracardiac neurones from adult rats. Resting membrane potential recorded 5 min after impalement was between −40 and −79 mV (−56·2 ± 1·7 mV, $n = 53$). Single or multiple action potential(s) could be induced by intracellular current pulse injections.

Inward rectifier current

All of the adult rat intracardiac neurones examined here showed a hyperpolarization-induced slow inward relaxation on the current trace and inward rectification on the current–voltage curve. Typical inward relaxations and current–voltage curves are shown in Fig. 2. Individual cells were initially voltage clamped at −60 mV, at which the holding current was normally close to zero. Hyperpolarizing commands evoked an instantaneous inward current followed by a slow inward relaxation and sometimes an inward tail current on returning to the holding potential (Figs 2*A* and 5*B*). This inward relaxation started at membrane potentials close to −70 mV and was clearly evident at −90 and −100 mV (Fig. 2). The amplitude and rate of the inward relaxation were increased as the command potential became more negative. As shown in Fig. 2*A*, the instantaneous current was larger at the end of the command than that recorded at the onset of the step, indicating an increase in membrane conductance during the 500 ms hyperpolarization. In some neurones, the current–voltage curve did not show obvious inward rectification in control Krebs solution (4·7 mM K^+) but was readily detectable in media containing elevated K^+ (15 mM) (Fig. 2). Reversal of the inward relaxation was not observed for voltage commands ranging from −60 to −150 mV in either 4·7 or 15 mM K^+.

The inward rectifier current was reversibly suppressed by Cs^+ (1 mM) in all twenty-six cells tested (Fig. 3*A*–*D*). The amplitude of the inward rectifier current was calculated by subtracting the steady-state inward relaxation in control Krebs solution from that in the presence of Cs^+ (Fig. 3*B*). At membrane potentials more positive than −80 mV, the inwardly rectifying current was zero. The amplitude was increased upon membrane hyperpolarization and reached a value of 450 ± 34 pA at −150 mV ($n = 6$). The threshold of the inward rectifier current was estimated visually from the divergence of the current–voltage curve before and after addition of Cs^+ ($n = 6$) (Fig. 3*B*). The mean activation threshold was −85·3 ± 2·2 mV ($n = 6$). Figure 3*C* shows that control current–voltage plots showed a linear instantaneous relationship and an inwardly rectifying steady-state curve, due to the activation of the inwardly relaxing current. Cs^+ (1 mM) suppressed both instantaneous and steady-state conductances, but the instantaneous conductance was reduced by 15–20%. Instantaneous conductance persisted when inward relaxation was completely inhibited by Cs^+, suggesting the existence of leak conductance in the absence of the inward rectifier

current. At the holding potential of −50 or −60 mV, Cs^+ (1 mM) did not change the holding current, suggesting that this current does not contribute significantly to the resting membrane potential in adult rat intracardiac neurones.

$BaCl_2$ in equimolar concentrations (1 mM) only slightly reduced the amplitude of inward relaxations at larger hyperpolarizations ($n = 6$, Fig. 3*E*), suggesting that the inward rectifier current in adult rat intracardiac neurones was more sensitive to Cs^+ than to Ba^{2+}. Ca^{2+}-free solution had little effect on inward rectifier current ($n = 13$, Fig. 3*F*). Addition of TEA (10 mM, $n = 11$, Fig. 3*F*), 4-AP (1–3 mM, $n = 8$, Fig. 3*F*) or muscarine (20 μM, $n = 5$, not shown) did not affect the inward relaxation.

The time course of the inward relaxation was examined (Fig. 4). Cells were subjected to a series of hyperpolarizing steps (500 ms) from the holding potential of −60 mV. The

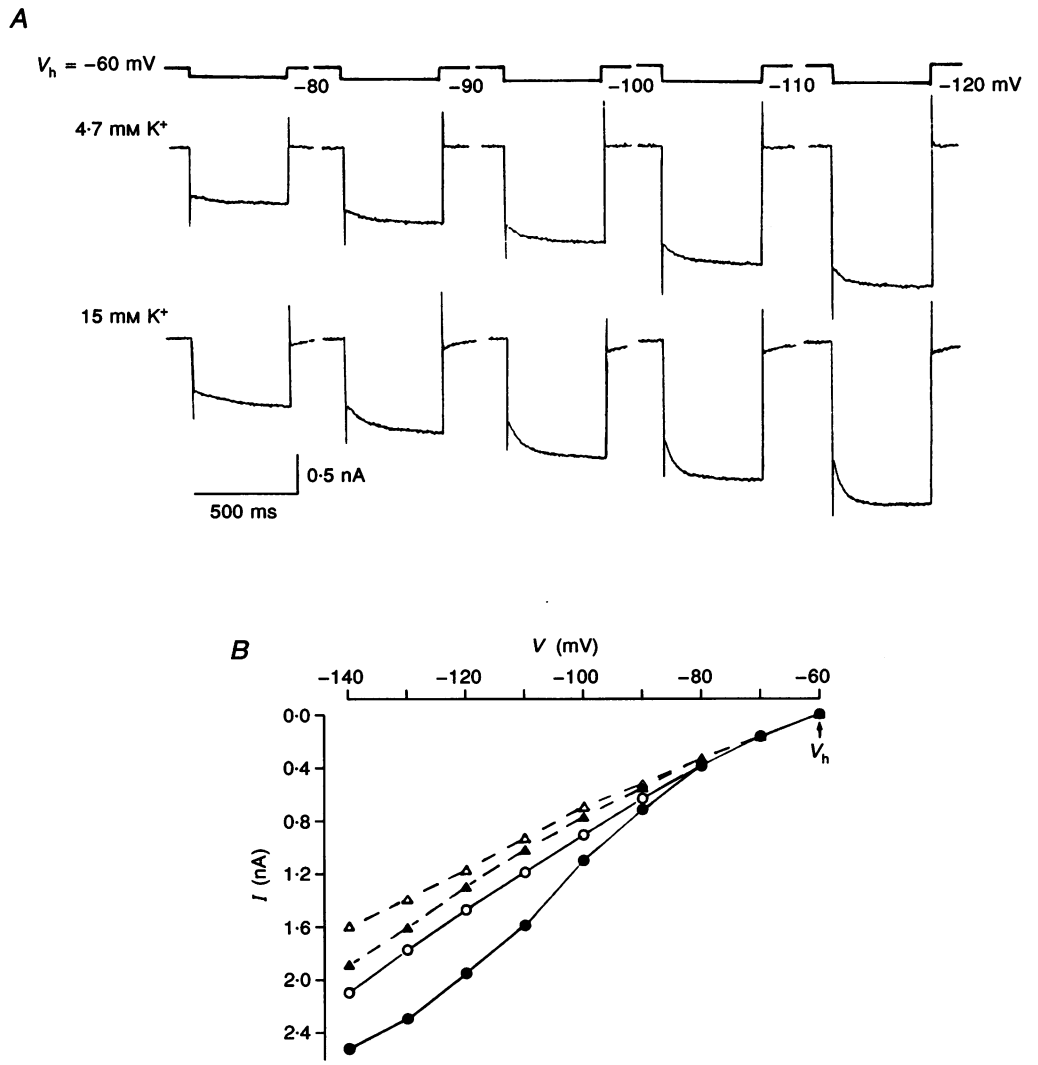

Figure 2. Hyperpolarization-activated slow time-dependent inward relaxation in an intracardiac neurone

A, from a holding potential (V_h) of −60 mV, step commands to −120 mV (10 mV increments, 500 ms pulse duration) induced a slow inward relaxation. On return to −60 mV, the instantaneous current was followed by a slow outward relaxation (more obvious in 15 mM $[K^+]_o$) as the inwardly rectifying current deactivated. Upper traces, command voltage steps. Middle traces, currents recorded in solution containing 4·7 mM $[K^+]_o$, 117 mM $[Na^+]_o$. Lower traces, currents recorded in solution containing 15 mM $[K^+]_o$, 98·4 mM $[Na^+]_o$. Note the increased amplitude and reduced time constant of relaxations in 15 mM $[K^+]_o$ (lower trace). *B*, the instantaneous (i; triangles) and steady-state (ss; circles) current–voltage relationship plotted from the data shown in *A*. Open symbols, 4·7 mM K^+; filled symbols, 15 mM K^+. Note the increase in inward rectification recorded in 15 mM $[K^+]_o$.

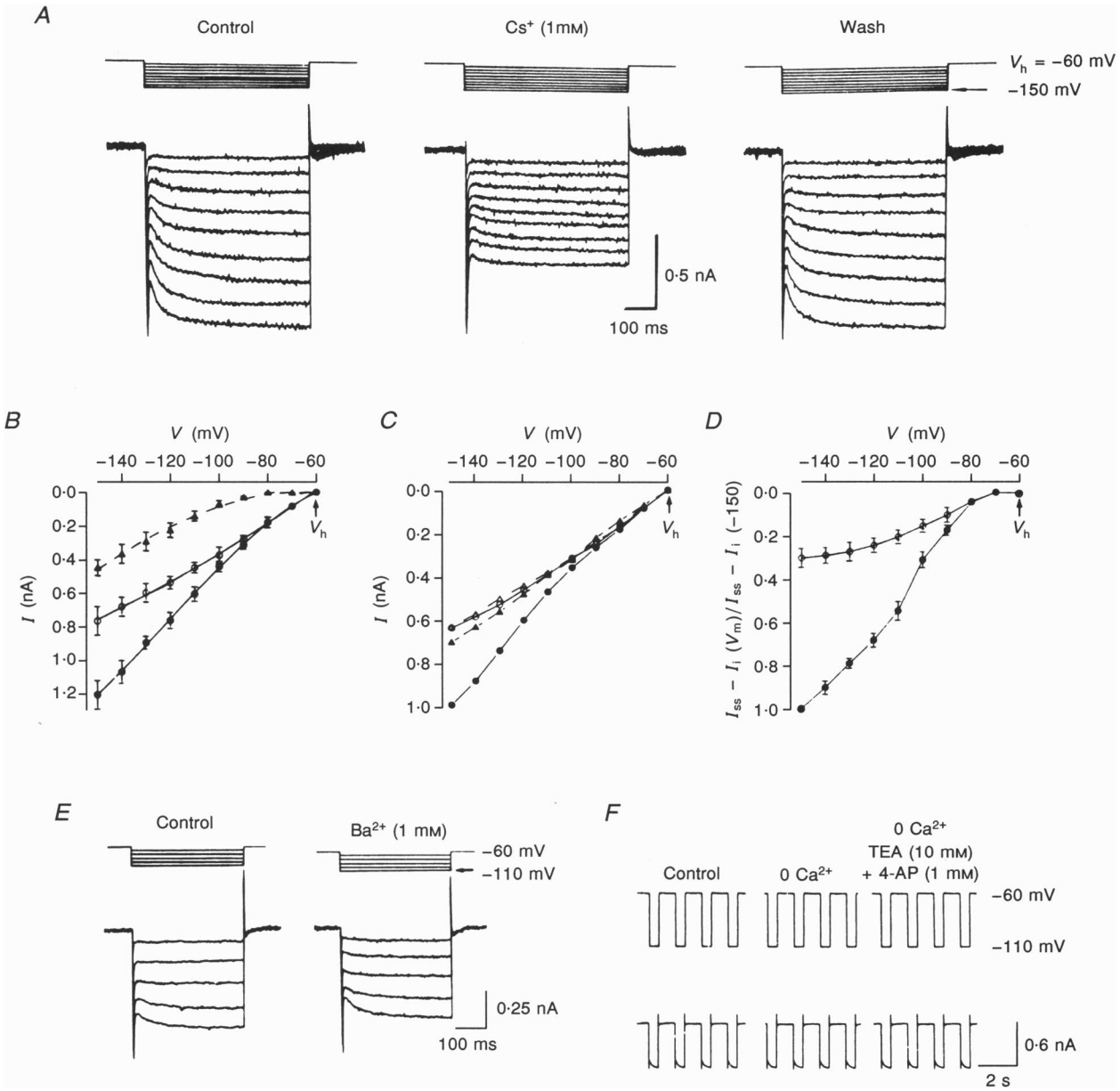

Figure 3. Pharmacological properties of the inwardly rectifying current

A, reversible blockade of inward relaxation and reduction in instantaneous (leak) current in the presence of 1 mM Cs^+. $V_h = -60$ mV; command potentials (V_c), −70 to −150 mV in 10 mV steps, 500 ms; this protocol was also used in *B*, *C* and *D*. *B*, current–voltage plot of the steady state of 6 neurones before (●) and during 1 mM Cs^+ superfusion (○). ▲, the difference between the two curves (means ± S.E.M.). *C*, example of the relationship of steady-state (ss; circles) and instantaneous (i; triangles) currents plotted against V_m in the presence (open symbols) and absence (filled symbols) of 1 mM Cs^+ for a single intracardiac neurone. *D*, plot of V_m against the inward relaxation amplitude (means ± S.E.M.) measured as the difference between the steady-state and instantaneous currents induced by stepping to V_m normalized for 6 cells with respect to control values on stepping to −150 mV from the holding potential of −60 mV, with (○) and without (●) Cs^+ (1 mM). *E*, Ba^{2+} (1 mM) slightly reduced inward relaxation recorded from a single neurone. $V_h = -60$ mV; steps, −70 to −110 mV in 10 mV increments, 500 ms. *F*, chart recording from a single cell to show that Ca^{2+}-free solution, TEA (10 mM) and 4-AP (1 mM) have little or no effect on inward relaxations (lower rows) evoked by steps from −60 to −110 mV (top rows).

inward relaxation from different voltage steps was normalized to 100% (I_0) and plotted as a function of time on a semilogarithmic scale. As shown in Fig. 4, the time course of inward relaxation was monoexponential. The time constants for inward relaxation calculated from six intracardiac neurones were 84·2 ± 5·8, 60·0 ± 4·4 and 41·3 ± 5·6 ms at −100, −110 and −120 mV, respectively. When fully activated, the current did not show any inactivation during the step commands for up to 2 s.

The contribution of Na^+ to the inward rectifier current was studied by replacing Na^+ with Tris. Na^+-free solution consistently reduced the fast Na^+ component of the action potentials and blocked the action potentials when Ca^{2+} was also removed from the perfusing solution (Fig. 5*A*). Removal of Na^+ from the medium with normal (4·7 mM) or high (15 mM) $[K^+]_o$ reversibly reduced the amplitude of the inward relaxation in all eleven neurones (Fig. 5*B*). The decrease of inward relaxation in Na^+-free solution was only slightly less in elevated $[K^+]_o$ (15 mM) as compared with control solution containing 4·7 mM $[K^+]_o$ (Fig. 5*Da* and *Db*). Addition of TTX (3 μM, $n = 3$, not shown) did not reduce the inward relaxation. The inward rectifier current was only partially eliminated in Na^+-free solution, and the remaining currents were largely suppressed by Cs^+ (1 mM, $n = 5$, not shown). The characteristics of the slowly activating inward rectifier current observed here are similar to the hyper- polarization-activated Na^+–K^+ current which may correspond to the previously reported Q-current (I_Q; Halliwell & Adams, 1982) or H-current (I_H; Hagiwara & Takahashi, 1974; Mayer & Westbrook, 1983).

Transient outward current (I_A)

Adult rat intracardiac neurones displayed a transient outward current that was activated by membrane depolarization from the potentials which were more negative with respect to the resting potential. The transient outward current or A-current (I_A; Rogawski, 1985), which was usually small in amplitude (< 1 nA) and brief in duration (< 100 ms), was elicited in twenty-four of thirty-two cells tested. Figure 6*Aa* shows the outward current present at −30 mV following the offset of a series of hyperpolarizing command pulses to −90 mV (also Fig. 7*A*). The amplitude of I_A increased as it was evoked from more negative potentials. I_A could also be evoked by depolarization pulses from a more negative holding potential (−90 mV in Fig. 6*Ab*). In this series of experiments, TTX (3 μM) was added to the superfusate, or

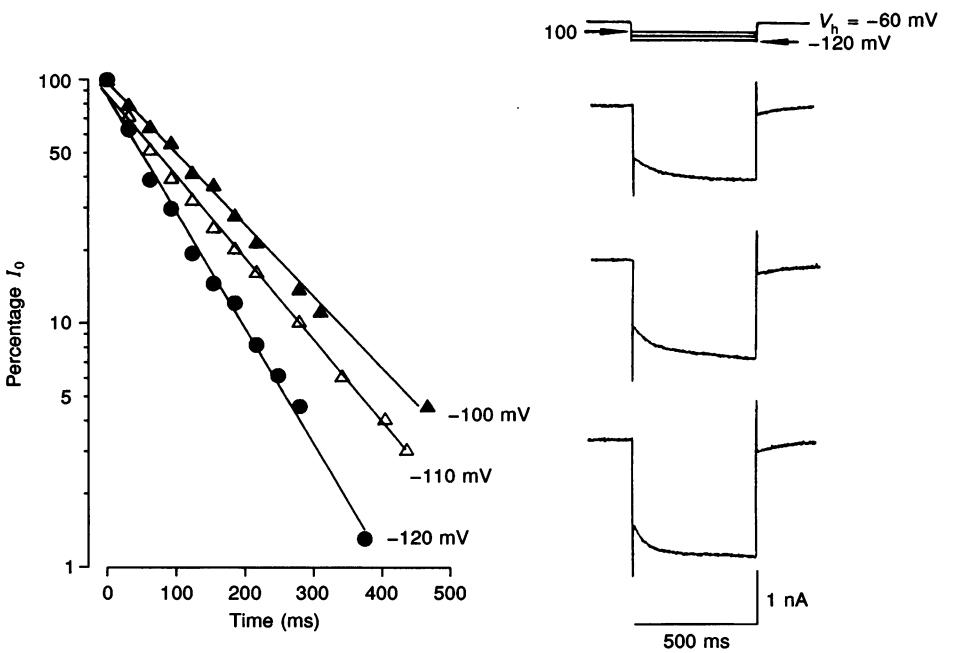

Figure 4. Kinetics of the inward relaxation underlying the time-dependent inwardly rectifying current

Inward relaxations of a single neurone (right) were evoked by steps (500 ms) from a V_h of −60 mV to −100, −110 and −120 mV. Relaxation time courses were plotted on a semilogarithmic graph (left). Lines were visually fitted. Correlation coefficients for the lines are 0·9983 (▲), 0·9985 (△) and 0·9986 (●). The zero-time intercept (I_0) was the difference between the instantaneous and steady-state values. The different values of I_0 were used to normalize data in each case. Current relaxations were expressed by a monoexponential, with the time constants of 80 (−100 mV), 58 (−110 mV) and 39 ms (−120 mV).

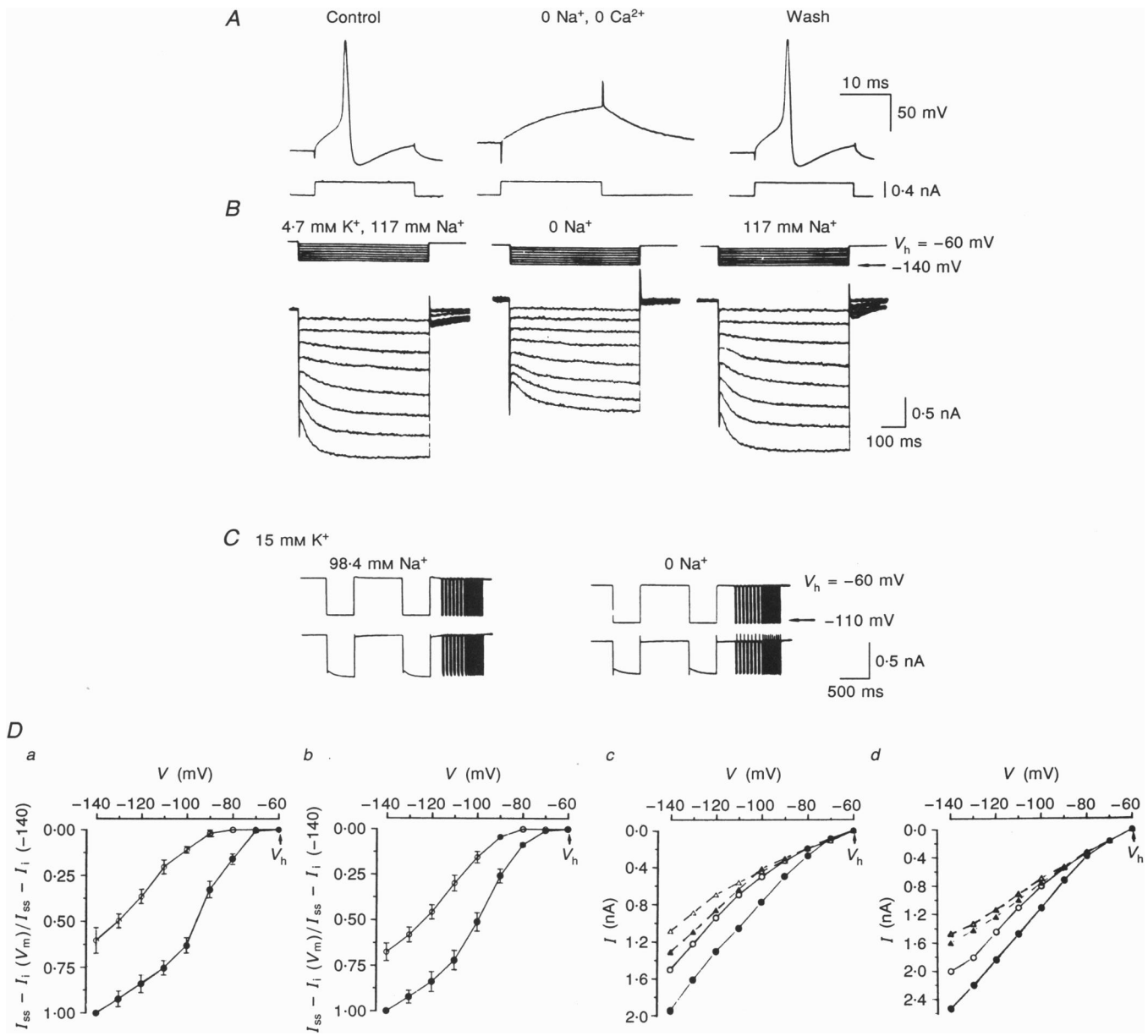

Figure 5. Effects of removal of Na^+ on inward rectifier current in an intracardiac neurone

A, action potential in an intracardiac neurone was reversibly blocked by a Na^+–Ca^{2+}-free solution. *B*, superfusion of Na^+-free solution reversibly reduced, but did not abolish, the inward relaxation and the tail current. $[K^+]_o = 4{\cdot}7$ mM, $[Na^+]_o = 117$ mM (in control). $V_h = -60$ mV; V_c, −70 to −140 mV in 10 mV increments, 500 ms. *C*, chart recording showing the reduction of inward relaxation (lower panels) by Na^+-free solution with elevated (15 mM) $[K^+]_o$. Voltage steps (top panels) from −60 to −110 mV. *Da*, differences between the steady-state and the instantaneous currents from 4 cells were plotted against V_m in control (●) and in Na^+-free solution (○). Data were normalized by the difference obtained in −140 mV and expressed as means ± S.E.M. $V_h = -60$ mV; V_c, −70 to −140 mV, 500 ms. $[K^+]_o = 4{\cdot}7$ mM, $[Na^+]_o = 117$ mM (in control). *Db*, a plot similar to *Da* from 5 cells but in elevated (15 mM) $[K^+]_o$ and Na^+-free solution. $[Na^+] = 98{\cdot}4$ mM in control. *Dc* and *Dd*, examples of raw plot of steady-state (ss; circles) and instantaneous (i; triangles) currents against V_m in the control (filled symbols) and Na^+-free solution (open symbols). Data were obtained in 4·7 $[K^+]_o$ (*Dc*) and 15 mM $[K^+]_o$ (*Dd*) solution from which data were pooled to obtain the graphs shown in *Da* and *Db*.

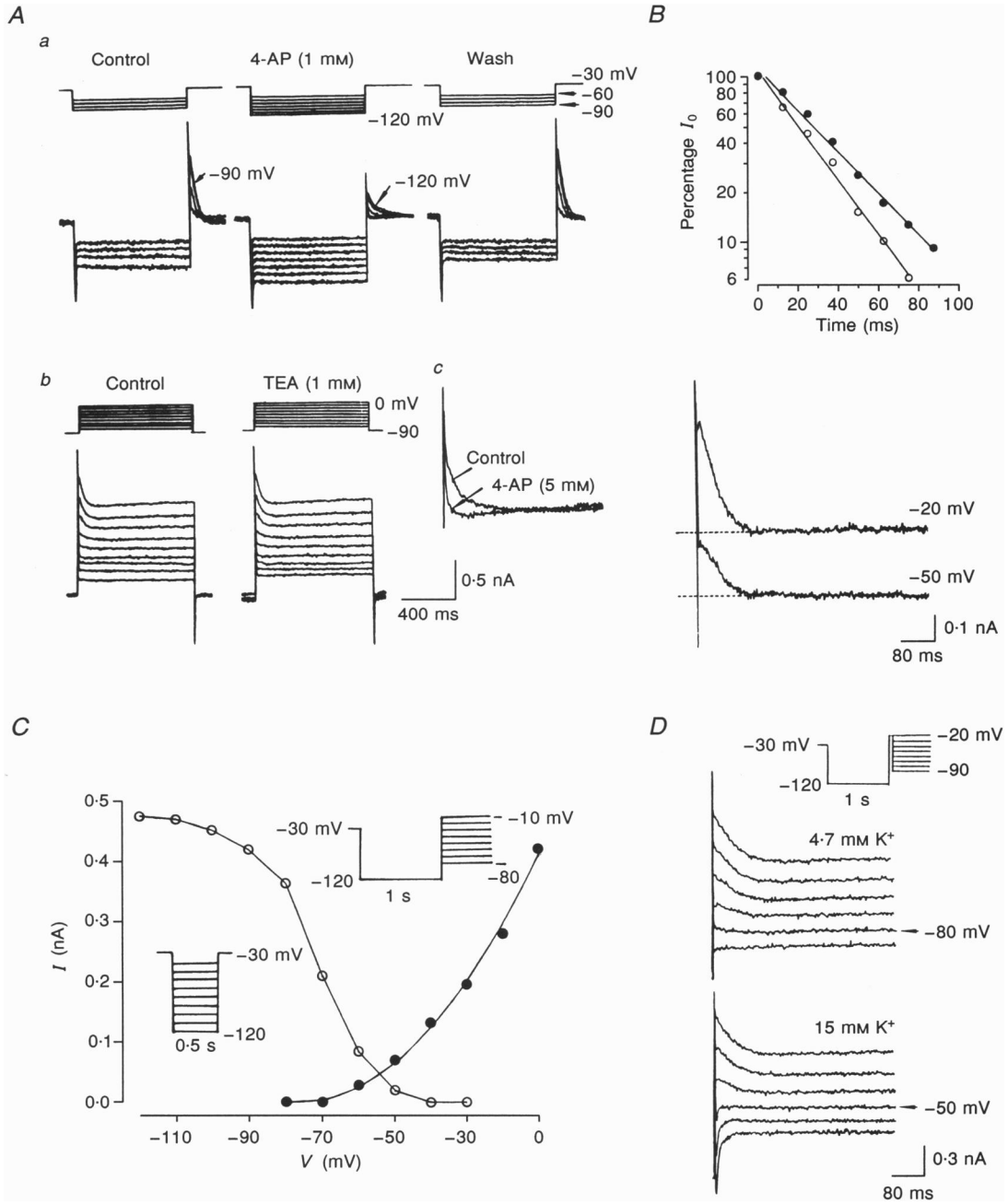

Figure 6. Effects of 4-AP and TEA on I_A in adult rat intracardiac neurones

A, I_A was evoked at −30 mV following step hyperpolarizations to −120 mV or by a series of depolarizing steps from −90 to 0 mV in 4 different cells. 4-AP (1 or 5 mM) attenuated but did not completely abolish I_A (*A a* and *A c*), especially when larger hyperpolarizations were applied (*A a*). TEA (10 mM) had no effect (*A b*). Ca^{2+}-free solution was used to eliminate $I_{K,Ca}$. *B*, time course of inactivation of I_A at −20 mV (○) and −50 mV (●) plotted on a semilogarithmic scale (inset); pre-pulse = −120 mV, 500 ms. The time constant for I_A inactivation was 20·3 (−20 mV) and 16·8 ms (−50 mV) in this neurone. Correlation coefficients of the lines are 0·9971 (○) and 0·9968 (●). *C*, the steady-state activation (●) and inactivation (○) curves for I_A. Data were obtained from an intracardiac neurone with a resting potential of −42 mV. See insets and text for experimental protocols. Currents were measured at their peak amplitude relative to baseline (○) or to the steady-state current at post-pulse termination (●). Curves were fitted by eye. *D*, reversal potential for I_A. See inset and text for the protocol. Only the currents during the post-pulse were presented. The interpolated reversal potentials for I_A in the experiment with 4·7 mM $[K^+]_o$ (upper part) and 15 mM $[K^+]_o$ (lower part) were −84·5 and −52·3 mV, respectively. The shift of reversal potential agreed with the predicted value of E_K from the Nernst equation. TTX (3 μM) was present in all the experiments shown (*A*–*D*).

Na^+-free solution was used to eliminate fast Na^+ current (Jones, 1987) and TEA (10 mM) to block the delayed rectifier K^+ current (I_{Kv}) and the Ca^{2+}-activated K^+ current ($I_{K,Ca}$) (Adams, Brown & Constanti, 1982*a*).

I_A displayed both voltage- and time-dependent inactivation. The inactivation time course of I_A was expressed monoexponentially with a time constant of 20·4 ± 1·5 ms at −50 mV and 15·8 ± 1·3 ms at −20 mV ($n = 4$, Fig. 6*B*). Inactivation usually appeared to be complete within 100 ms. Longer hyperpolarization command pulses produced larger I_A tails as inactivation was progressively removed at hyperpolarized potentials. The time constant for the removal of inactivation was determined by using a series of command pulses to −120 mV from the holding potential of −30 mV. The duration of the command pulse varied from 10 ms to 1 s. The peak I_A seen upon repolarization to −30 mV was plotted as a function of the command pulse duration (not shown) (Connor & Stevens, 1971*a*; Adams *et al.* 1982*a*). The time constant for removal of inactivation was 20·0 ± 2·1 ms ($n = 3$). The activation kinetics were too fast to be resolved using the single-electrode voltage-clamp technique; current peaked within 5 ms of command onset or offset. The steady-state activation and inactivation curves of I_A were studied with a

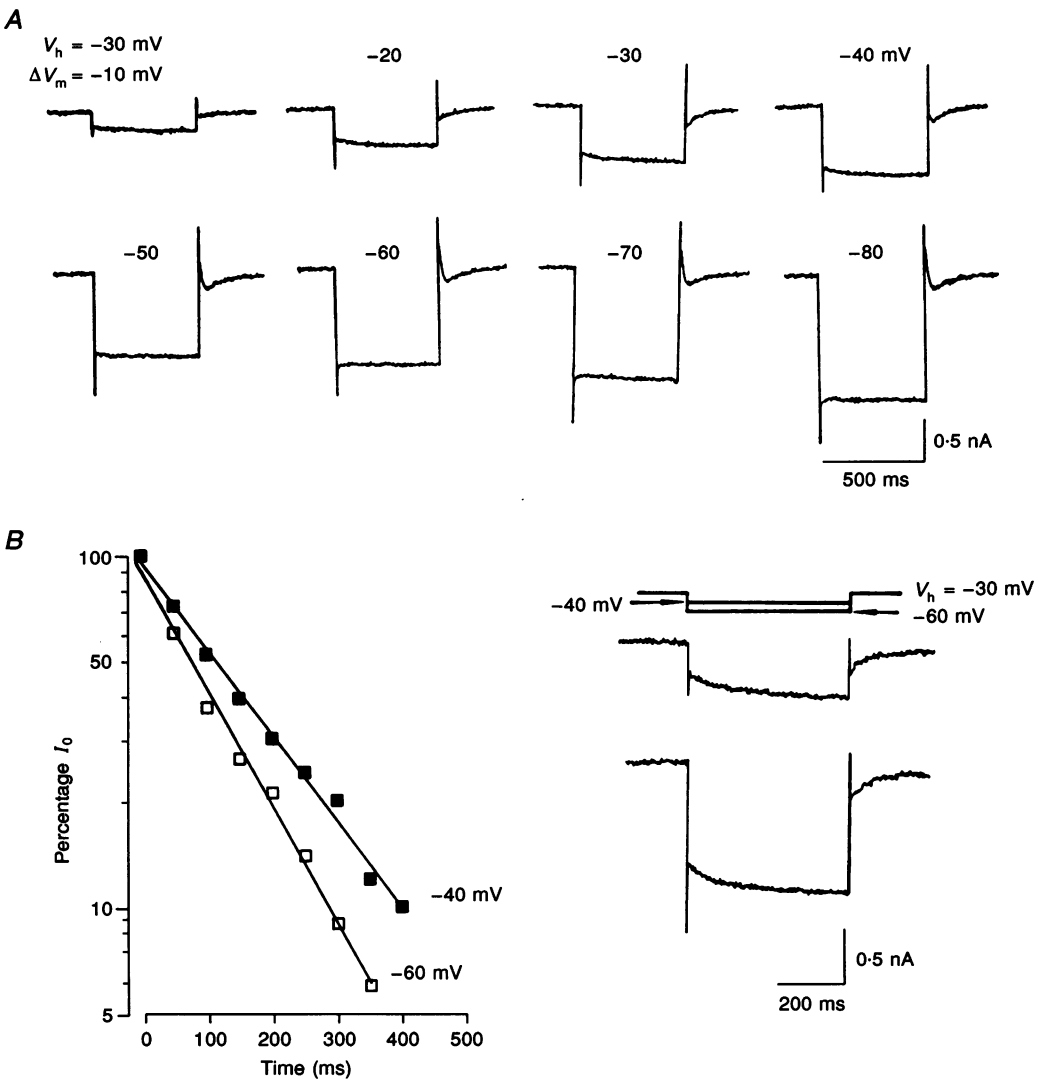

Figure 7. Detection of I_M in a rat intracardiac neurone

A, membrane currents elicited by step hyperpolarizations from a V_h of −30 mV. I_M relaxations are visible during smaller hyperpolarizations, and I_A follows larger (≥ −70 mV) steps. TTX (3 μM) was present throughout this experiment. *B*, left, relaxation time course of I_M plotted on a semilogarithmic scale.For definition of I_0 see legend of Fig. 4. I_M relaxations fitted a single exponential with relaxation time constants of 50·8 ms at −40 mV (■) and 78·7 ms at −60 mV (□). Lines are fitted by eye to data for cell shown on right. Correlation coefficients for the lines are 0·9971 (□) and 0·9964 (■). Right, I_M relaxations evoked by step hyperpolarizations from −30 mV to −40 and −60 mV. TTX (3 μM) and 4-AP (1 mM) were present throughout experiment *B*.

conventional protocol (see the insets of Fig. 6*C*). The membrane potential was clamped to −30 mV. For the activation curve, the pre-pulse was −120 mV and the post-pulse was between −80 and −10 mV. The peak I_A was plotted as a function of the post-pulse voltage. For the inactivation curve, a series of hyperpolarizing potentials (between −120 and −40 mV) were commanded and the currents flowing upon returning to −30 mV were measured. The peak I_A was plotted as a function of the hyperpolarizing potential. Steady-state inactivation was removed at potentials more negative than −40 mV and the threshold voltage for activation was about −70 mV (Fig. 6*C*). The two curves show a small overlap between −70 and −40 mV (Fig. 6*C*). Similar results were observed in another two cells.

The amplitude of I_A was decreased in Krebs solution with elevated K^+. Figure 6*D* shows the effects of $[K^+]_o$ on the reversal potential of I_A. Inactivation was removed by stepping to −120 mV for 1 s and I_A was activated by

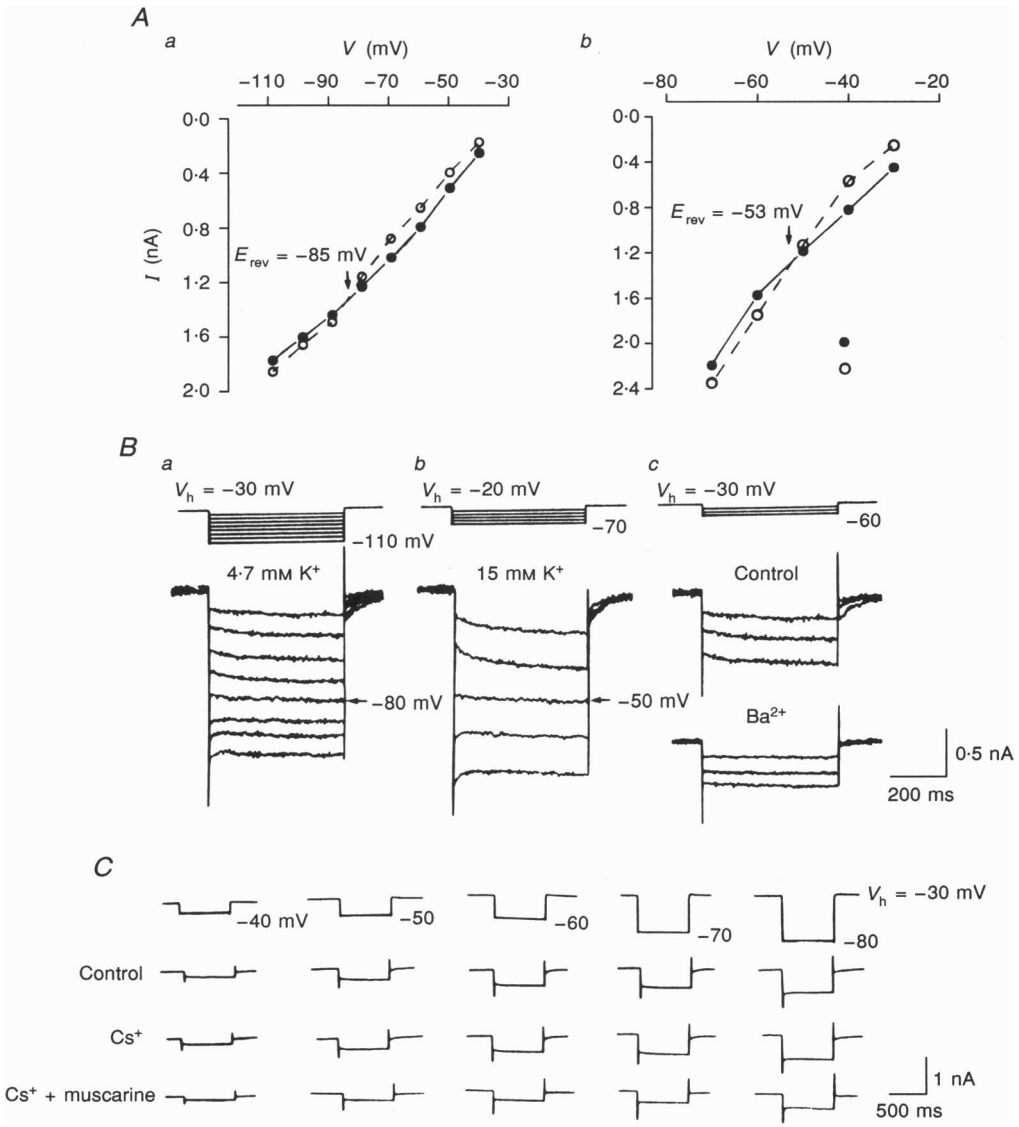

Figure 8. Properties of I_M in intracardiac neurones

A, reversal potential (E_{rev}) for I_M. Instantaneous (i, ○) and steady-state (ss, ●) currents were plotted as a function of step hyperpolarizations. *A a*, $[K^+]_o$ = 4·7 mM, V_h = −30 mV, E_{rev} = −85 mV; *A b*, $[K^+]_o$ = 15 mM, V_h = −20 mV, E_{rev} = −53 mV. Lines are fitted by eye to data for cell shown in *Ba* and *Bb*. *B*, progressive decrease in amplitude and reversal of I_M relaxations as step hyperpolarizations increased from the holding potential in different $[K^+]_o$ (4·7 and 15 mM). Reduction of I_M relaxation by Ba^{2+} (2 mM) is shown in *Bc*. *C*, lack of effect of 1 mM Cs^+ on I_M relaxations and their blockade by muscarine (10 μM). V_h = −30 mV (see top line). All experiments were carried out in the presence of TTX (3 μM) and 4-AP (1 mM).

transiently returning to the holding potential of −30 mV. The potential was then stepped to different post-pulses during the resulting I_A (see inset). Since the current reversed its polarity at the membrane potential close to E_K in all three cells tested, I_A results from an increase in K^+ conductance (Fig. 6*D*).

Some of the pharmacological properties of I_A are shown in Fig. 6*A*. In all seven cells tested, 4-AP (1 mM) reversibly reduced the amplitude of I_A by about 80% in three cells (Fig. 6*A a*) and abolished the current in another four cells. At higher concentrations (3–5 mM), 4-AP consistently blocked I_A (Fig. 6*A c*). I_A was not eliminated in a solution containing TEA (10 mM; Fig. 6*A b*) or Cs^+ (1 mM).

M-current (I_M)

To study this current, neurones were voltage clamped at a relatively depolarized membrane potential (−25 to −30 mV) and subjected to a series of hyperpolarizing command steps (500 ms, 10 mV increments) in the presence of TTX (3 μM). At this depolarized voltage range, I_M could be easily separated from the inward rectifier current, which flows only when the membrane potential was more negative than −80 mV. Figure 7*A* shows a typical experiment in which the membrane was stepped from −30 mV to more negative levels; two membrane currents were revealed. At the onset of each voltage command, an instantaneous inward current step was followed by a much slower inward relaxation. On return to the holding potential, the instantaneous current was reduced and followed by a slow outward relaxation. This small reduction of the instantaneous current on return to the holding potential indicates a decrease of membrane conductance during the 500 ms command. With larger hyperpolarizations, the inward relaxation first became smaller and faster and then

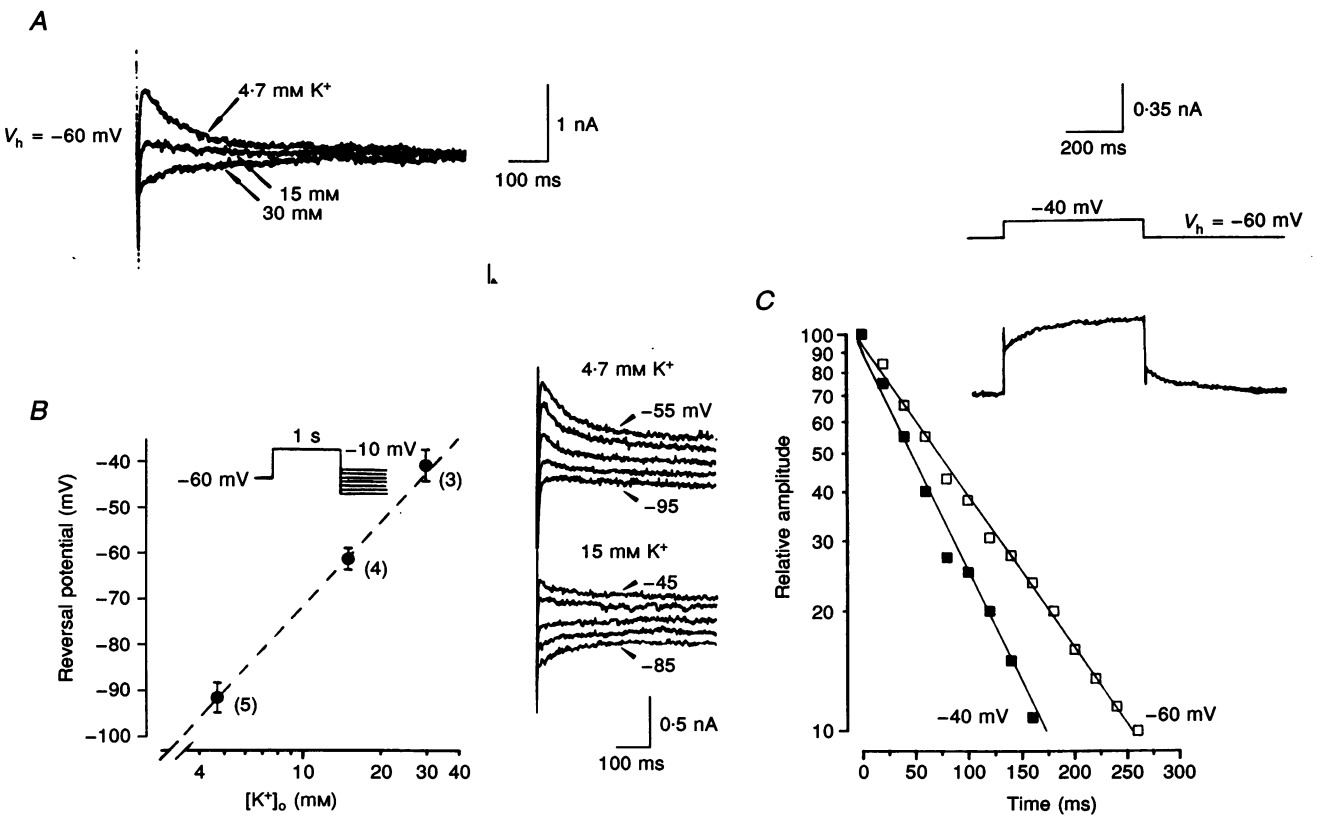

Figure 9. Depolarization-induced outward K^+ currents in an intracardiac neurone

A, deactivating tail current of depolarization-induced outward K^+ current after repolarization from −20 mV at three $[K^+]_o$ (4·7, 15 and 30 mM) from a single neurone. V_h = −60 mV. *B*, dependence of the reversal potential of tail current on $[K^+]_o$. An example of the tail current recorded at different $[K^+]_o$ from a single cell is shown to the right. Inset of the graph shows the voltage protocol. Reversal potentials (means ± S.E.M.) were plotted against the $\log[K^+]_o$. *C*, time course of the activation (■) and deactivation (□) of the depolarization-activated outward K^+ current. For the activation time course, the zero-time intercept was the difference between the steady-state and the instantaneous values. For deactivation time course, instantaneous tail current was taken as 100. Lines were visually fitted. Time courses expressed monoexponentially with the activation time constant of 75 ms and deactivation time constant of 58 ms. Data were taken from the recording shown in the inset. All experiments were carried out in the presence of TTX (3 μM), Ba^{2+} (1 mM) and 4-AP (1 mM).

reversed at about −85 mV. On return to the holding potential, the slow outward relaxation was interrupted by a transient outward current (I_A) which was increased as the membrane became more hyperpolarized. The slow inward and outward relaxations are characteristics of the deactivation and reactivation of the non-inactivating, time- and voltage-sensitive potassium current, I_M (Adams *et al.* 1982*a*). 4-AP (1–3 mM) was used in the following studies to remove the influence of I_A.

I_M was detected in 90% (37/41) of the intracardiac neurones tested. The deactivation time course of I_M was monoexponential with a time constant of 48·5 ± 5·4 ms at −60 mV and 79·3 ± 4·6 ms at −40 mV ($n = 5$, Fig. 8*B*). Figure 8*Aa*, *Ab*, *Ba* and *Bb* shows the dependence of the reversal potential of inward relaxation on $[K^+]_o$. Both the steady-state and instantaneous currents at different K^+ concentrations were plotted as a function of the step command (Fig. 8*A*). The intersection of the steady-state and instantaneous curves represents the estimated reversal potential for I_M relaxation. The mean reversal potentials in $[K^+]_o$ of 4·7 and 15 mM were −85·2 ± 1·2 ($n = 12$) and −53·1 ± 1·9 mV ($n = 5$), respectively. These values of reversal potential for I_M relaxation fit well with the E_K predicted from the Nernst equation, suggesting potassium ions as the carrier of I_M.

As found in other vertebrate neurones (Adams *et al.* 1982*a*; Adams *et al.* 1982*b*; Allen & Burnstock, 1990*a*), application of muscarine (10 μM) reversibly blocked I_M in intracardiac neurones ($n = 4$, Fig. 8*C*). Addition of Ba^{2+} (1 mM) also decreased the amplitude of I_M ($n = 3$, Fig. 8*Bc*). Cs^+ (1 mM), which reduced inward rectifier current, had no effect on I_M ($n = 7$, Fig. 8*C*).

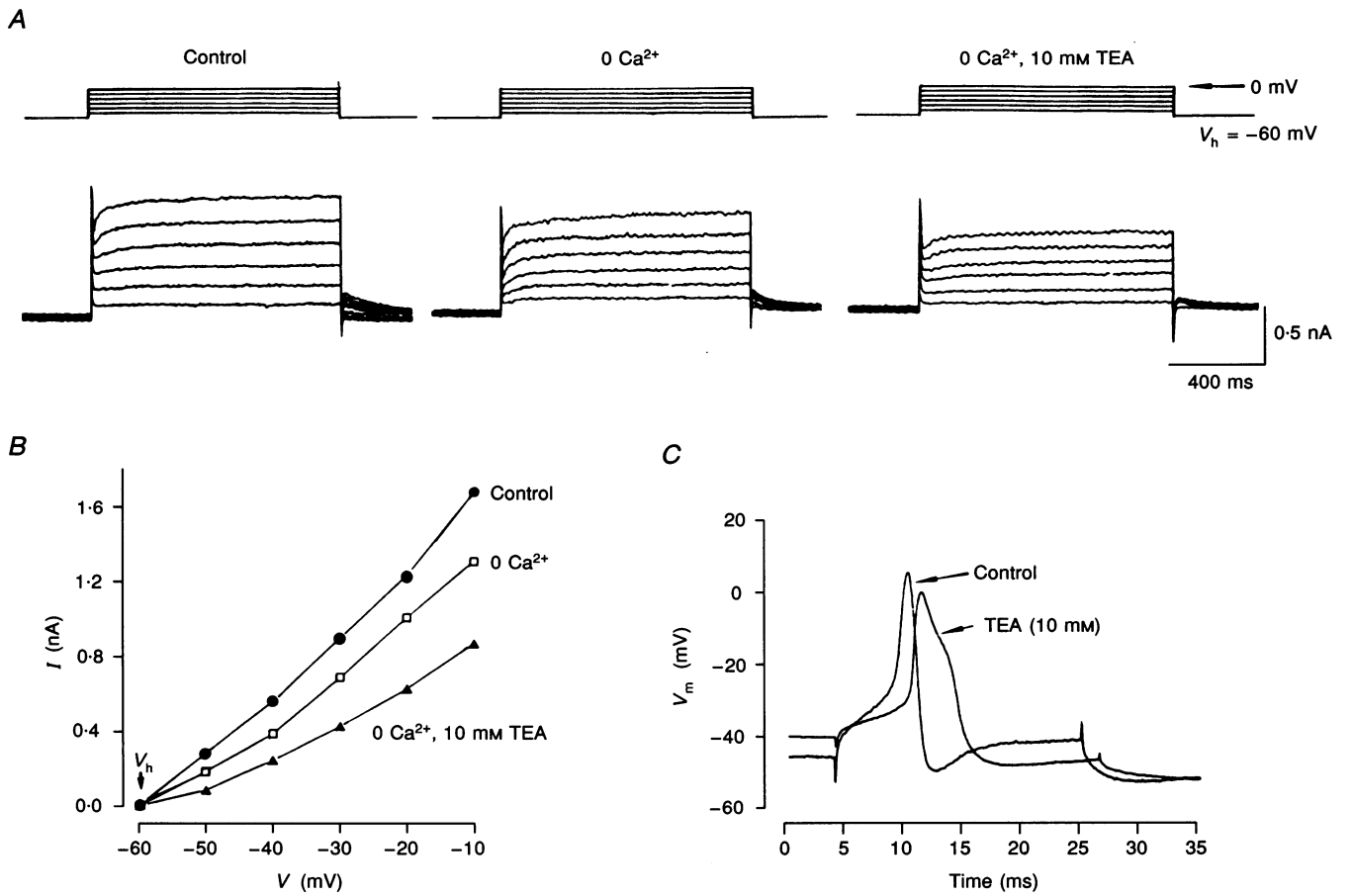

Figure 10. Detection of I_K and $I_{K,Ca}$ in an intracardiac neurone

A, the depolarization-activated outward relaxation and the tail current were first decreased by removing Ca^{2+} from the media and then further depressed by addition of TEA (10 mM) in a single neurone. $V_h = -60$ mV; V_c, −50 to −10 mV in 10 mV increments, 1 s. *B*, current–voltage relationship from a different neurone shows the presence of Ca^{2+}-sensitive and Ca^{2+}-insensitive outward K^+ currents. Voltage protocol shown in *A*. *C*, effects of TEA (10 mM) on the resting potential, action potential and after-hyperpolarization from a single intracardiac neurone. Experiments *A* and *B* were carried out in the presence of TTX (3 μM), Ba^{2+} (1 mM) and 4-AP (1 mM).

Depolarization-activated outward currents

In adult rat intracardiac ganglion cells, depolarizing commands (10–50 mV, 1 s) from the holding potential of −60 mV, which was close to the resting potential, activated a slowly developing outward relaxation with an outward tail current upon repolarization (Figs 9 and 10*A*). All experiments were carried out in the presence of TTX (3 μM), Ba^{2+} (1 mM) and 4-AP (1 mM).

The amplitude of the deactivating tail current varied with $[K^+]_o$ (Fig. 9*A*). The amplitude of the steady-state outward relaxation was reduced in increased $[K^+]_o$. Reversal potentials for the tail current in different $[K^+]_o$ were determined by presenting the neurones post-pulses (range, −35 to −95 mV) immediately after the 1 s depolarization pre-pulse (from −60 to −10 mV, see inset of Fig. 9*B*). The outward tail current became smaller as the post-pulses were made more hyperpolarized and eventually reversed its polarity at $-92{\cdot}2 \pm 4{\cdot}0$ mV in 4·7 mM $[K^+]_o$ ($n = 5$, Fig. 9*B*). The reversal potential shifted to $-61{\cdot}0 \pm 3{\cdot}3$ mV ($n = 4$) and $-41{\cdot}8 \pm 4{\cdot}2$ mV ($n = 3$) when $[K^+]_o$ was increased to 15 and 30 mM, respectively (Fig. 9*B*). The best-fit straight line (by least-squares method) in Fig. 9*B* had a slope of 60·8 mV for a tenfold change in $[K^+]_o$, indicating that the depolarization-activated outward currents were carried by K^+ ions.

The outward relaxation developed monoexponentially with a time constant of 74 ± 5 ms at −40 mV ($n = 6$, Fig. 9*C*). Fully activated outward K^+ current did not show obvious inactivation during the step command for 1 s. The deactivating time constant of tail current fitted a monoexponential function and was 110 ± 9 ms at −60 mV ($n = 6$, Fig. 9*C*).

Depolarization-activated outward K^+ currents and their tail currents recorded in the presence of Ba^{2+}, TTX and 4-AP were reduced in a Ca^{2+}-free solution and were further reduced by the addition of TEA (10 mM); the effects were reversible ($n = 3$, Fig. 10*A* and *B*). In current-clamp mode, superfusion of TEA (10 mM) depolarized the resting membrane potential by about 5–8 mV ($n = 7$). The rate of the action potential repolarization and the amplitude of the after-hyperpolarization (AHP) were also markedly decreased (Fig. 10*C*). These results suggested that in adult rat intracardiac neurones, the depolarization-activated outward K^+ currents may contain both the delayed rectifier K^+ current (I_{Kv}) and the Ca^{2+}-activated K^+ current ($I_{K,Ca}$).

Discharges induced by K^+-channel blockers

The following series of experiments were carried out to evaluate the role of K^+ currents in the initiation of rhythmic discharges. Hexamethonium (100 μM) was routinely included in the Krebs solution to eliminate fast excitatory postsynaptic potentials (EPSPs).

Bath application of TEA (10 mM) initiated repetitive discharges in five of the seven neurones examined; an

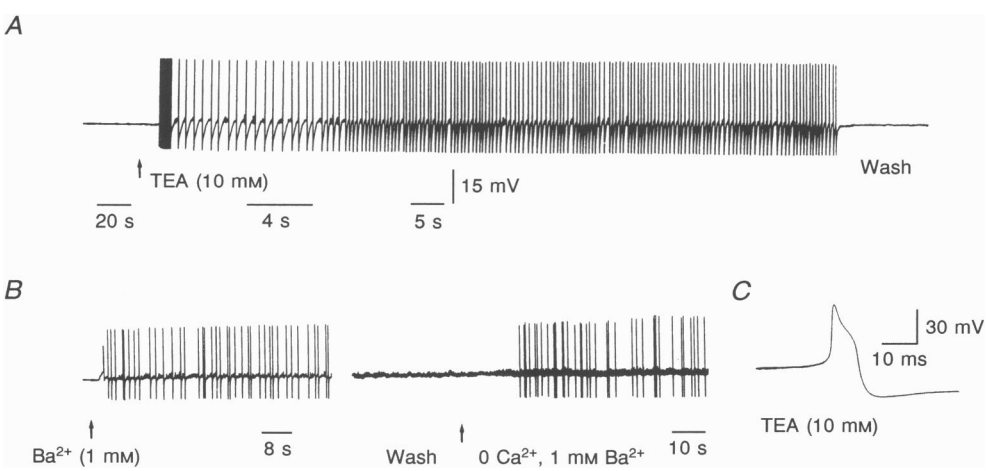

Figure 11. Potassium channel blockers initiated repetitive discharges in rat intracardiac neurones

A, superfusion of TEA (10 mM) reversibly induced repetitive firing. The discharge was regular with a frequency of ~2·3 Hz. Recording was made from a quiescent neurone in the presence of hexamethonium (100 μM). *B*, Ba^{2+} (1 mM) reversibly initiated repetitive discharge, which was not blocked by Ca^{2+}-free solution in a neurone with a resting potential of −53 mV. The first and second arrows indicate the perfusion of Ba^{2+} and Ca^{2+}-free plus Ba^{2+} solution, respectively. *C*, action potential initiated by TEA (10 mM). Note the 'shoulder' on repolarizing phase. Recordings were from the same neurone as in *A*. The amplitude of action potentials in *A* and *B* was truncated due to the limited frequency response of the pen recorder.

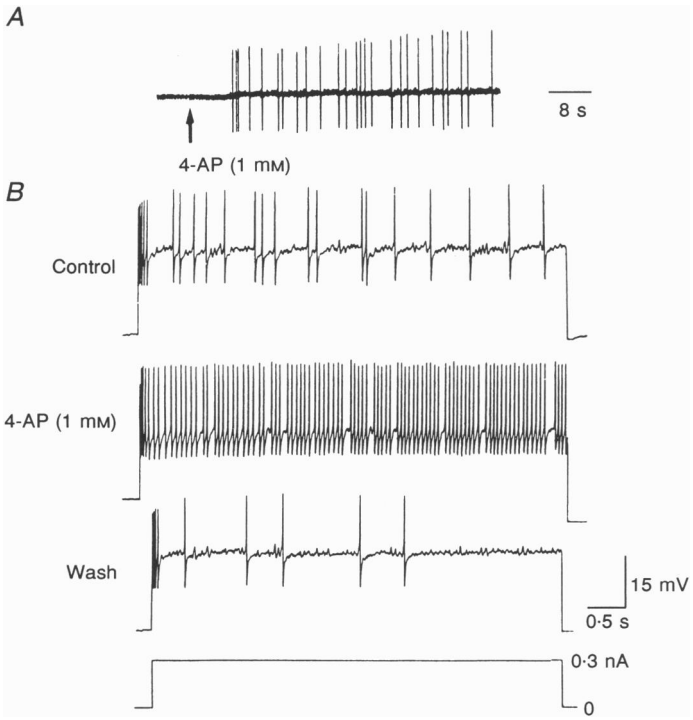

Figure 12. Effects of 4-AP on intracardiac neurone excitability

A, superfusion of 4-AP (1 mM) initiated spontaneous discharge in a quiescent cell with a resting potential of −47 mV in the presence of hexamethonium (100 μM). *B*, prolonged depolarizing pulse (6 s, 0·3 nA, bottom row) evoked repetitive discharges (top row). The frequency of discharges was significantly and reversibly increased by superfusion of 4-AP (1 mM, second and third rows) in a quiescent neurone with a resting potential of −55 mV. The amplitude of spike potentials was truncated.

example is shown in Fig. 11*A*. Within 1 min after arrival of TEA in the bath, the cell started to discharge continuously, and the effect was reversible within 5 min after washing with Krebs solution. As would be expected, TEA prolonged the repolarizing phase of action potentials (Fig. 11*C*). The rhythmic activity was probably not due to the small depolarizing effect of TEA, as the repetitive discharge was not abolished by momentarily returning the membrane potential to the resting level nor initiated by depolarizing the membrane to the same level by current injections in the absence of TEA.

Ba^{2+} (1 mM) induced repetitive discharge in three of the seven otherwise quiescent neurones (Fig. 11*B*). The discharge was of an irregular pattern and not abolished in a Ca^{2+}-free solution (Fig. 11*B*).

Bath application of 4-AP (1 mM) initiated repetitive firings in three of the seven neurones; one of the experiments is shown in Fig. 12*A*. A second type of response was noted in another five neurones whereby injection of a prolonged depolarizing current pulse evoked multiple spike discharges, and 4-AP increased the discharge frequency in these neurones. An example is illustrated in Fig. 12*B*; this neurone displayed frequency adapation as the first few spikes at the beginning of the depolarization had a higher frequency.

Cs^{2+} (1 mM) did not cause repetitive firing or increase firing frequency in any of the ten intracardiac neurones studied.

DISCUSSION

The present experiments indicate that adult rat intracardiac neurones exhibit, in addition to a slowly activating, inwardly rectifying Na^+–K^+ current, at least four types of K^+ conductances: (1) transient outward current (I_A), (2) M-current (I_M), (3) delayed rectifier current (I_{Kv}) and (4) a Ca^{2+}-activated K^+ current ($I_{K,Ca}$).

Inwardly rectifying current

That hyperpolarization-activated membrane conductance produces a region of inward rectification in the steady-state current–voltage relationship has been found in many biological membranes. The inward rectifier of marine eggs (Hagiwara & Takahashi, 1974) and olfactory cortex neurones (Constanti & Galvan, 1983) is a K^+-specific current with V–E_K-dependent activation kinetics (Hagiwara, Miyazaki & Rosenthal, 1976; Constanti & Galvan, 1983). Barium and Cs^+ are equally effective in blocking this current (Hagiwara *et al.* 1976; Constanti & Galvan, 1983). The inward rectifier in the sino-atrial nodes (DiFrancesco & Ojeda, 1980), Purkinje fibres (DiFrancesco, 1981) and various neurones (Mayer & Westbrook, 1983; Tokimasa & Akasu, 1990) is specific to K^+ and Na^+ and blocked by Cs^+ but not Ba^{2+}; the activation kinetics are not V–E_K dependent (Mayer & Westbrook, 1983; Tokimasa & Akasu, 1990). The inward rectifier in the parasympathetic neurones of rat trachea has the properties of the inward rectifier found in marine eggs and sino-atrial nodes (Allen

& Burnstock, 1990*b*). In the adult rat intracardiac neurones, the properties of the inward rectifier (e.g. being $[K^+]_o$ and $[Na^+]_o$ dependent, being Cs^+ sensitive and Ba^{2+} resistent, and not reversing the polarity near E_K) resemble those of the inward rectifier Na^+–K^+ current or the so-called I_H, I_Q and I_F described in the egg cells, sino-atrial node and vertebrate neurones (Hagiwara & Takahashi, 1974; DiFrancesco & Ojeda, 1980; Halliwell & Adams, 1982; Mayer & Westbrook, 1983). In addition to the I_Q-like current, the possibility that intracardiac neurones may exhibit a fast, time-independent, Cs^+- and Ba^{2+}-sensitive inward rectification similar to that reported in guinea-pig basal forebrain neurones (Griffith, 1986) cannot be excluded. The significance of I_H in neuronal membrane is unclear. It has been suggested in photoreceptors and sensory neurones that I_H prevents the cell membrane from over-hyperpolarization and consequently keeps the membrane potential in a range suitable for the action and release of neurotransmitters (Mayer & Westbrook, 1983; Fain & Lisman, 1992).

Properties of I_A

The characteristics of I_A in intracardiac neurones appear comparable to those observed in a variety of other neurones in its voltage dependence of steady-state activation and inactivation, kinetics and pharmacological properties (Connor & Stevens, 1971*a*; Akasu & Tokimasa, 1989; Galligan, North & Tokimasa, 1989). Our experiments have shown that, in addition to diminishing I_A, 4-AP (1 mM) increased the frequency of repetitive firing and initiated spontaneous spikes in some intracardiac neurones. It seems likely that I_A in the adult rat intracardiac neurones acts to slow repetitive discharge by reducing the rate of decay of the AHP (Connor & Stevens, 1971*b*). Since the presence of I_A synchronizes the firing rate with the stimulus intensity (degree of depolarization) in a graded fashion (Rogawski, 1985), intracardiac neurones may have the prerequisite property of neural integration. It is of interest to note that I_A and inward rectifier current appear to be absent in the cultured intracardiac neurones from neonatal rats (Xu & Adams, 1992). I_A also appears to be absent in the majority of frog intracardiac neurones (Selyanko, Zidichouski & Smith, 1992). Whether the presence or absence of this current is of developmental and/or physiological significance has yet to be examined.

Properties of I_M

The I_M identified in the adult rat intracardiac neurones has features similar to that first reported in B cells of frog lumbar sympathetic ganglia (Brown & Adams, 1980) and later in several central and peripheral neurones (Brown, 1988). Since both I_M and inward rectifier current are present in the same intracardiac neurones, these two currents may counterbalance each other near the resting membrane potential (Mayer & Westbrook, 1983; Allen & Burnstock, 1990*b*). Thus, I_M exerts a hyperpolarizing influence and is activated upon membrane depolarization, whereas the inward rectifier promotes membrane depolarization and is activated upon membrane hyperpolarization. However, the activation threshold of inward rectifier in intracardiac neurones (−70 mV) is more negative than the resting potential (about −60 mV) and the activation threshold in some autonomic (Allen & Burnstock, 1990*b*; Tokimasa & Akasu, 1990) and sensory (Mayer & Westbrook, 1983) neurones. It seems likely that the function of inward rectifier current is to drive the membrane potential back to near the resting level when membrane is markedly hyperpolarized. A similar activation threshold of inward rectifier is reported in myenteric spike after-hyperpolarization neurones (Galligan *et al.* 1989). In addition, to function as a gain control, I_M may be involved in muscarinic synaptic transmission (Brown, 1988; Allen & Burnstock, 1990*a*; Xi-Moy, Randall & Wurster, 1993). Cholinergic slow excitatory postsynaptic potentials have been recorded in canine intracardiac ganglion neurones (Xi-Moy *et al.* 1993). Inhibition of I_M by Ba^{2+} in adult rat intracardiac neurones initiates tonic firing. It can be surmised that I_M in mammalian intracardiac neurones may have multiple physiological roles.

Properties of outward K^+ current

In addition to I_M, the depolarization-activated outward K^+ currents in adult rat intracardiac neurones appear to consist of two components: Ca^{2+}-insensitive I_{Kv} and Ca^{2+}-sensitive $I_{K,Ca}$. Outward K^+ currents of similar characteristics have also been identified in cultured neonatal rat intracardiac neurones; the $I_{K,Ca}$, however, appears to be activated in a more depolarized range (Xu & Adams, 1992). The effects of I_{Kv} and $I_{K,Ca}$ on action potential repolarization and AHP were clearly observed when they were blocked by TEA. I_{Kv} is primarily involved in the repolarization phase, as the latter is not affected by the Ca^{2+} channel blocker. The magnitude and duration of the AHP are regulated by both I_{Kv} and $I_{K,Ca}$, as TEA caused an additional reduction of the amplitude of AHP after administration of Ca^{2+}-free solution (see also Xu & Adams, 1992). Inhibition of I_{Kv} and $I_{K,Ca}$ exerts an important role in facilitating sustained spike discharge (Tanaka & Kuba, 1987). Superfusion of Ca^{2+}-free solution in rat intracardiac neurones caused a small membrane depolarization (Selyanko, 1992), indicating that $I_{K,Ca}$ may be involved in the regulation of resting membrane potential. The background K^+ current may also contribute to the resting potential in the bullfrog sympathetic and cultured parasympathetic intracardiac neurones (Jones, 1989; Xu & Adams, 1992).

K^+ channel blockers

The observation that several K^+ channel blockers, e.g. TEA, Ba^{2+} and 4-AP, can initiate repetitive discharge in otherwise quiescent intracardiac neurones suggests that K^+ currents may represent the important inhibitory conductances that normally prevent the initiation of spontaneous intrinsic activity. In lobster stomatogastric ganglia, a Ca^{2+}-activated K^+ current is likely to be responsible for the inhibition of spontaneous bursting in normally silent neurones (Harris-Warrick & Johnson, 1987). In both the guinea-pig and canine intracardiac ganglia, inhibition of M-current initiated spontaneous spikings in quiescent cells (Allen & Burnstock, 1990*a*; Xi *et al.* 1992). Are there intrinsic modulatory inputs which may inactivate the inhibitory or shunting conductances, thereby leading to spontaneous firing in intracardiac neurones? Several putative transmitters or modulators have been reported to initiate spontaneous firings in various neurones, e.g. dopamine and serotonin in lobster stomatogastric ganglion (Flamm & Harris-Warrick, 1986*a*, *b*) and muscarinic agonists in mammalian intracardiac ganglia (Allen & Burnstock, 1990*a*; Xi *et al.* 1992). The possible existence of multiple interactions among individual conductances and between the intrinsic conductances and the modulatory inputs (Grace & Bunney, 1984*a*, *b*; Goh, Kelly & Pennefather, 1989; Shepard & Bunney, 1991) may explain the variability encountered in intracardiac ganglia where some of the intracardiac neurones exhibit no repetitive discharges to potassium channel blockade and others do. It is also possible that either the endogenous discharge in some of these unresponsive cells is inhibited by some other mechanisms or some of the conductances supporting the endogenous discharge are absent.

In summary, the K^+ conductances described here are similar to those described in other mammalian neurones (Akasu & Tokimasa, 1989; Allen & Burnstock, 1990*b*; Xu & Adams, 1992). As shown in other neurones, the K^+ currents identified in adult rat intracardiac neurones may play a multiple role in neuronal excitability by regulating the resting membrane potential, action potential configuration and rhythmic discharge. As a corollary, the various K^+ currents acting in concert may enable the parasympathetic intracardiac neurones to function as the peripheral integrator in vagal regulation of cardiac function.

Adams, P. R., Brown, D. A. & Constanti, A. (1982*a*). M-currents and other potassium currents in bullfrog sympathetic neurones. *Journal of Physiology* **330**, 537–572.

Adams, P. R., Brown, D. A. & Constanti, A. (1982*b*). Pharmacological inhibition of the M-current. *Journal of Physiology* **332**, 223–262.

Akasu, T. & Tokimasa, T. (1989). Potassium currents in submucous neurones of guinea-pig caecum and their synaptic modification. *Journal of Physiology* **416**, 571–588.

Allen, T. G. J. & Burnstock, G. (1990*a*). M1 and M2 muscarinic receptors mediate excitation and inhibition of guinea-pig intracardiac neurones in culture. *Journal of Physiology* **422**, 463–480.

Allen, T. G. J. & Burnstock, G. (1990*b*). A voltage-clamp study of the electrophysiological characteristics of the intramural neurones of the rat trachea. *Journal of Physiology* **423**, 593–614.

Brown, D. A. (1988). M-currents: an update. *Trends in Neurosciences* **11**, 294–299.

Brown, D. A. & Adams, P. R. (1980). Muscarinic suppression of a novel voltage-sensitive K current in a vertebrate neurone. *Nature* **283**, 673–676.

Burkholder, T., Chambers, M., Hotmire, K., Wurster, R. D., Moody, S. & Randall, W. C. (1992). Gross and microscopic anatomy of the vagal innervation of the rat heart. *Anatomical Record* **232**, 444–452.

Connor, J. A. & Stevens, C. F. (1971*a*). Voltage clamp studies of a transient outward membrane current in gastropod neural somata. *Journal of Physiology* **213**, 21–30.

Connor, J. A. & Stevens, C. F. (1971*b*). Prediction of repetitive firing behaviour from voltage clamp data on an isolated neurone soma. *Journal of Physiology* **213**, 31–53.

Constanti, A. & Galvan, M. (1983). Fast inward-rectifying current accounts for anomalous rectification in olfactory cortex neurones. *Journal of Physiology* **335**, 153–178.

DiFrancesco, D. (1981). A study of the ionic nature of the pacemaker current in calf Purkinje fibres. *Journal of Physiology* **314**, 377–393.

DiFrancesco, D. & Ojeda, C. (1980). Properties of the current I_f in the sino-atrial node of the rabbit composed with those of the current I_{k2} in Purkinje fibres. *Journal of Physiology* **308**, 353–367.

Fain, G. L. & Lisman, J. E. (1992). Membrane conductances of photoreceptors. *Progress in Biophysics and Molecular Biology* **37**, 91–147.

Flamm, R. E. & Harris-Warrick, R. M. (1986*a*). Aminergic modulation in lobster stomatogastric ganglion. I. Effects on motor pattern and activity of neurons within the pyloric circuit. *Journal of Neurophysiology* **55**, 847–865.

Flamm, R. E. & Harris-Warrick, R. M. (1986*b*). Aminergic modulation in lobster stomatogastric ganglion. II. Target neurons of dopamine, octopamine and serotonin within the pyloric circuit. *Journal of Neurophysiology* **55**, 866–881.

Galligan, J. J., North, R. A. & Tokimasa, T. (1989). Muscarinic agonists and potassium currents in guinea-pig myenteric neurones. *British Journal of Pharmacology* **96**, 193–203.

Goh, J. W., Kelly, M. E. M. & Pennefather, P. S. (1989). Electrophysiological function of the delayed rectifier (I_k) in bullfrog sympathetic ganglion neurones. *Pflügers Archiv* **413**, 482–486.

Grace, A. A. & Bunney, B. S. (1984*a*). The control of firing pattern in nigral dopaminergic neuron: single spike firing. *Journal of Neuroscience* **4**, 2866–2876.

Grace, A. A. & Bunney, B. S. (1984*b*). The control of firing pattern in nigral dopaminergic neurons: burst firing. *Journal of Neuroscience* **4**, 2877–2890.

Griffith, W. H. (1986). Membrane properties of cell types within guinea pig basal forebrain nuclei *in vitro*. *Journal of Neurophysiology* **59**, 1590–1612.

HAGIWARA, S., MIYAZAKI, S. & ROSENTHAL, N. P. (1976). Potassium current and the effect of caesium on this current during anomalous rectification of the egg cell membrane of a starfish. *Journal of General Physiology* **67**, 621–638.

HAGIWARA, S. & TAKAHASHI, K. (1974). The anomalous rectification and cation selectivity of the membrane of a starfish egg cell. *Journal of Membrane Biology* **18**, 61–80.

HALLIWELL, J. V. & ADAMS, P. R. (1982). Voltage-clamp analysis of muscarinic excitation in hippocampal neruons. *Brain Research* **250**, 71–92.

HARRIS-WARRICK, R. M. & JOHNSON, B. R. (1987). Potassium channel blockade induces rhythmic activity in a conditional burster neuron. *Brain Research* **416**, 381–386.

HASSALL, C. J. S. & BURNSTOCK, G. (1986). Intrinsic neurones and associated cells of the guinea-pig heart in culture. *Brain Research* **364**, 102–113.

JONES, S. W. (1987). Sodium currents in dissociated bull-frog sympathetic neurones. *Journal of Physiology* **389**, 605–627.

JONES, S. W. (1989). On the resting potential of isolated frog sympathetic neurons. *Neuron* **3**, 153–161.

MALOR, R., TAYLOR, S., CHESHER, G. B. & GRIFFIN, C. J. (1974). The intramural ganglia and chromaffin cells in guinea pig atria: an ultrastructural study. *Cardiovascular Research* **8**, 731–744.

MAYER, M. L. & WESTBROOK, G. L. (1983). A voltage-clamp analysis of inward (anomalous) rectification in mouse spinal sensory ganglion neurones. *Journal of Physiology* **340**, 19–45.

MORAVEC, M. & MORAVEC, J. (1984). Intrinsic innervation of the atrioventricular junction of the rat heart. *American Journal of Anatomy* **171**, 307–319.

RANDALL, W. C. (1984). Selective autonomic innervation of the heart. In *Nervous Control of Cardiovascular Function*, ed. RANDALL, W. C., pp. 46–67. Oxford University Press, New York.

ROGAWSKI, M. A. (1985). The A-current: how ubiquitous a feature of excitable cell is it? *Trends in Neurosciences* **8**, 214–219.

SELYANKO, A. A. (1992). Membrane properties and firing characteristics of rat cardiac neurons *in vitro*. *Journal of the Autonomic Nervous System* **39**, 181–190.

SELYANKO, A. A., ZIDICHOUSKI, J. A. & SMITH, P. A. (1992). The effects of muscarine and adrenaline on patch-clamped frog cardiac parasympathetic neurones. *Journal of Physiology* **443**, 355–370.

SHEPARD, P. D. & BUNNEY, B. S. (1991). Repetitive firing properties of putative dopamine-containing neuron *in vitro*: regulation by an apamin-sensitive Ca^{2+}-activated K^+ conductance. *Experimental Brain Research* **86**, 141–150.

TANAKA, K. & KUBA, K. (1987). The Ca^{2+}-sensitive K^+ currents underlying the slow after-hyperpolarization of bull-frog sympathetic neurons. *Pflügers Archiv* **410**, 234–242.

TOKIMASA, T. & AKASU, T. (1990). Cyclic AMP regulates an inward rectifying sodium–potassium current in dissociated bull-frog sympathetic neurones. *Journal of Physiology* **420**, 409–429.

WEIHE, E., REINECKE, M. & FORSSMANN, W. G. (1984). Distribution of vasoactive intestinal polypeptide-like immunoreactivity in the mammalian heart – interrelation with neurotensin- and substance P-like immunoreactive nerves. *Cell and Tissue Research* **236**, 527–540.

XI, X., RANDALL, W. C. & WURSTER, R. D. (1991*a*). Morphology of intracellularly labeled canine intracardiac ganglion cells. *Journal of Comparative Neurology* **314**, 396–402.

XI, X., RANDALL, W. C. & WURSTER, R. D. (1991*b*). Intracellular recordings from canine intracardiac ganglion cells. *Journal of the Autonomic Nervous System* **32** 177–182.

XI-MOY, S. X. & DUN, N. J. (1992). Potassium currents in adult rat intracardiac neurons *in situ*. *Society for Neuroscience Abstracts* **18**, 1181.

XI-MOY, S. X., RANDALL, W. C. & WURSTER, R. D. (1993). Nicotinic and muscarinic synaptic transmission in canine intracardiac ganglion cells innervating sino-atrial nodal region. *Journal of the Autonomic Nervous System* **42**, 201–214.

XU, Z. J. & ADAMS, D. J. (1992). Resting membrane potential and potassium currents in cultured parasympathetic neurones from rat intracardiac ganglia. *Journal of Physiology* **456**, 405–424.

Acknowledgements

We wish to thank Dr Peter Smith for helpful comments on the manuscript and Chong Ren for preparing the figures. This work was supported by a Postdoctoral Fellowship to S.X.M. from the American Heart Association Ohio Affiliate and by NIH Grant NS18710 from the Department of Health and Human Services.

Author's present address

S. X. Xi-Moy: Department of Pharmacology, East Tennessee State University, James H. Quillen College of Medicine, Johnson City, TN 37614, USA.

Received 10 January 1994; accepted 12 December 1994.